Scattering resonances in two-dimensional crystals with application to graphene

V. U. Nazarov, E. E. Krasovskii, and V. M. Silkin

Scattering resonances in two-dimensional crystals with application to graphene

V. U. Nazarov

*Research Center for Applied Sciences, Academia Sinica, Taipei 11529, Taiwan**

E. E. Krasovskii and V. M. Silkin

Departamento de Física de Materiales, Facultad de Ciencias Químicas,
Universidad del País Vasco/Euskal Herriko Unibertsitatea,
Apdo. 1072, San Sebastián/Donostia, 20080 Basque Country, Spain
Donostia International Physics Center (DIPC), Paseo Manuel de Lardizabal 4,
San Sebastián/Donostia, 20018 Basque Country, Spain and
IKERBASQUE, Basque Foundation for Science, 48011 Bilbao, Spain

We address the band-structure of two-dimensional crystals above the vacuum level in the context of discrete states immersed in the three-dimensional continuum. Scattering resonances are discovered that originate from the coupling of the in-plane and perpendicular motions, as elucidated by the analysis of an exactly solvable model. Some of the resonances turn into true bound states at high-symmetry **k** vectors. *Ab initio* scattering theory verifies the existence of the resonances in realistic graphene and shows that they lead to a total reflection of the incident electron below and total transmission above the resonance energy.

Electronic structure of single layer crystals has attracted much attention due to the discovery of graphene[1] and other atomically thin systems (boron nitride[2], silicene[3]). Graphene is the most popular material because it combines the unique electronic properties with technological robustness, which makes it especially promising for nanoelectronics[4]. Its most exciting feature – the linear dispersion of the highest occupied π and lowest empty π^* bands – is known since 1947, when Wallace[5] obtained it analytically in a tight-binding model. The bound electronic states of the free-standing graphene have been recently addressed in a number of *ab initio* studies[6–11], so its low energy band structure is presently well understood.

At energies above the vacuum level we enter the continuous spectrum due to the infinite motion perpendicular to the layer, as shown in Fig. 1 for the band-structure of graphene. Some of the lines entering the continuum from below are seen to retain their individuality inside the continuous spectrum. Their origin is clear: They correspond to the states of an in-plane motion but with the energy above the continuum edge. However, at a deeper level, a fundamental issue arises: An electron moving with a sufficiently high energy within the layer and parallel to it has, generally speaking, a non-zero probability to escape into vacuum, which would impart this state a finite life-time, i.e., turn it into a resonance. The presence of the resonances in the band-structure of 2D crystals above the vacuum level as exemplified by graphene is the main message of this Rapid Communication. We argue that those resonances are of special kind: They originate from the coupling of two motions, of which one is across the layer under the action of the layer's confining potential well and another is in the layer's plane in a periodic 2D lattice potential, *each of those potentials separately supporting no resonances.* We will also show that some of the discrete levels retain zero linewidth, by this being true bound states immersed into continuum.

The discrete levels within the continuous spectrum deserve close attention because they strongly affect optical absorption in the UV range, as well as electron photoexcitation and propagation toward the detector in a photoemission experiment. Recent experimental progress in angle-resolved photoemission (ARPES) on epitaxial[12–17] and suspended[18,19] graphene, as well as in low energy electron diffraction (LEED)[20,21] calls for a detailed understanding of its electronic structure at higher energies.
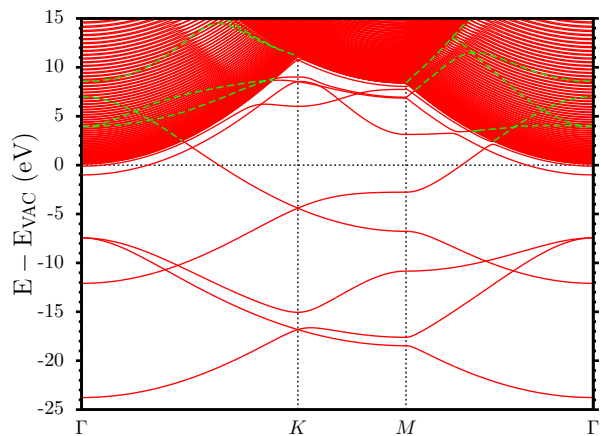

FIG. 1. (color online) Band-structure of graphene obtained in the repeated super-cell geometry. The all-electron full-potential linearized augmented-plane wave code *Elk*[22] was used for this calculation. The separation between the periodically stacked layers is $d = 400$ bohr. The energy axis zero is at the vacuum level at Γ point.

We start by considering a trivial case: Let us have a quantum well $V(z)$ in z direction with the flat potential in xy plane. Then, if the well supports a bound state, and since the two perpendicular motions are independent in this case, the 3D wave-function is a product of a bound

state in z direction and a plane wave in the xy plane. As a result, there exist states which are bound to the well while having an arbitrarily high energy above the vacuum level due to the motion in xy plane. If, however, we apply a potential that is periodic in xy plane, the variables in the Schrödinger equation do not separate any more, i.e., the two perpendicular motions become coupled. To get a better insight on how this affects the high-lying energy bands of the in-plane motion, we first introduce a model which is exactly solvable and at the same time retains all the basic physics involved:

δ-function quantum well with laterally periodic potential – We are looking for a solution of the Schrödinger equation

$$\left[-\frac{1}{2}\Delta + V(z, \mathbf{r}_\parallel)\right]\psi(z, \mathbf{r}_\parallel) = E\psi(z, \mathbf{r}_\parallel) \qquad (1)$$

with the model potential being a product of a periodic function in the xy plane and the δ-function quantum well in z direction

$$V(z, \mathbf{r}_\parallel) = \sum_{\mathbf{G}} V_{\mathbf{G}} e^{i\mathbf{G}\cdot\mathbf{r}_\parallel}\,\delta(z), \qquad (2)$$

where $\mathbf{G}$ are the 2D reciprocal lattice vectors. We set $V_0 < 0$ to ensure the existence of a state bound to the $z = 0$ plane. The solutions of Eq. (1) with the potential (2) can be written explicitly as Bloch waves with respect to the motion in the xy plane

$$\psi(z, \mathbf{r}_\parallel) = \sum_{\mathbf{G}} a_{\mathbf{G}} e^{i\sqrt{2E - (\mathbf{G}+\mathbf{k})^2}\,|z|} e^{i(\mathbf{G}+\mathbf{k})\cdot\mathbf{r}_\parallel}, \qquad (3)$$

where $\mathbf{k}$ is the in-plane wave-vector within the first Brillouin zone, and $a_{\mathbf{G}}$ are still unknown coefficients. Importantly, in Eq. (3) we have retained the exponent with one sign only, which selects out bound and resonant states[23], if the latter exist, while omitting the scattering states propagating in the z direction[24]. The jump in the wavefunction's z-derivative $\psi'(z, \mathbf{r}_\parallel)$ is obtained by the integration of Eq. (1) in z over the infinitesimal interval $[0_-, 0_+]$

$$\psi'(0_+, \mathbf{r}_\parallel) - \psi'(0_-, \mathbf{r}_\parallel) = 2\sum_{\mathbf{G}} V_{\mathbf{G}} e^{i\mathbf{G}\cdot\mathbf{r}_\parallel}\psi(0, \mathbf{r}_\parallel). \qquad (4)$$

Together, Eqs. (3) and (4) lead to the system of equations for the coefficients $a_{\mathbf{G}}$

$$\sum_{\mathbf{G}'} V(\mathbf{G} - \mathbf{G}')a_{\mathbf{G}'} = i\sqrt{2E - (\mathbf{G} + \mathbf{k})^2}\, a_{\mathbf{G}}. \qquad (5)$$

The crucial point is the choice of the sign of the square roots in Eqs. (3) and (5). Denoting the generic square root by s, the rule is: Re $s > 0$ if Re $s^2 > 0$ and Im $s > 0$ otherwise, which choice ensures the correct asymptotic behavior of the necessarily normalizable and the necessarily non-normalizable wave-functions, of the bound states and resonances, respectively[23].

The values of E which allow for non-zero solutions of the homogeneous system of linear equations (5) determine the band-structure of our model system. However, in contrast to the original set-up of Eq. (1), Eqs. (5) constitute a *nonlinear eigenvalue problem*[25] for the energies E. We emphasize that this fundamental difference comes from the fact that the separation of the bound and resonant states from those of continuum has been already achieved in Eq. (5).
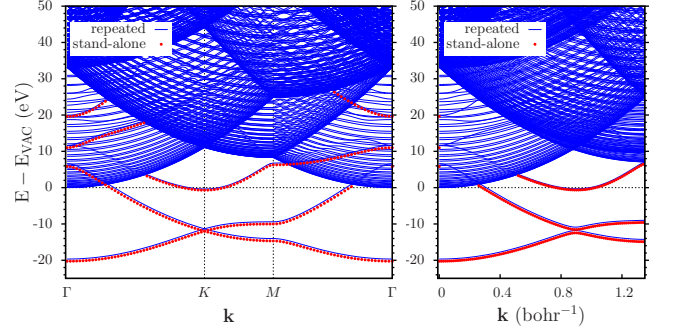

FIG. 2. (color online) Left: Band-structure of the model system obtained with the repeated super-cell geometry calculation (blue lines) and with solving the eigenvalue problem (5) for a stand-alone plane (red points). The calculation has been conducted along $\Gamma - K - M - \Gamma$ line. Right: The same for the asymmetric direction of $\mathbf{k}$ along $7\mathbf{b}_1 + 13\mathbf{b}_2$, where $\mathbf{b}_1$ and $\mathbf{b}_2$ are the primitive reciprocal vectors. The energy axis zero is at the vacuum level at Γ point.

In Fig. 2, results of the numerical solution of the non-linear eigenvalue problem (5), which give the band-structure of the stand-alone layer, are presented together with the results of calculations carried out for the same system in the repeated super-cell geometry. The symmetry of the 2D periodic potential is chosen that of the honeycomb lattice, graphene's lattice constant is used, and the values of the Fourier coefficients of the potential are: $V_0 = -0.7|\mathbf{b}|$ and $V_{\mathbf{G}} = 0.1|\mathbf{b}|$ for the first $\mathbf{G}$ star, and $V_{\mathbf{G}} = 0$ otherwise, $\mathbf{b}$ being the primitive vector of the reciprocal lattice. In the left panel, the wave-vector varies along the $\Gamma - K - M - \Gamma$ lines while in the right panel an asymmetric direction of $\mathbf{k}$ is chosen. For the bands below the vacuum edge, both the repeated-geometry and the stand-alone calculations yield the identical results regardless of the symmetry of the wave-vector. In contrast, above the vacuum edge, whether or not a particular state localized near $z = 0$ survives as a true bound state is determined by the symmetry of its $\mathbf{k}$ point. For the asymmetric case of $\mathbf{k}$, there are no such states. As can be seen from Fig. 2, along the high-symmetry directions some of the bound state bands do survive. Moreover, an isolated high-lying bound state exists at the Γ point at the energy of ≈ 83 eV (not shown in Fig. 2). The 2D crystal, thus, presents a simple and instructive example of bound states in the continuum, very different from the known cases of atoms[26] or quantum dots[27].

While the results in Fig. 2 establish the existence of

TABLE I. Eigenenergies (in eV) for the model system obtained with the reduced size of $V(\mathbf{G}-\mathbf{G}')$ matrix permitting the fully analytical solution of the non-linear eigenvalue problem (5).

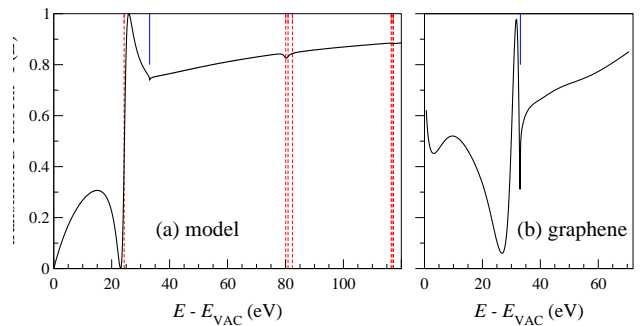| Γ	K	M
-20.3	-11.9	-13.9
5.8	-0.6	-9.5
11.0	26.0 - 0.2 i	7.7
19.6	26.8 - 0.6 i	9.8 - 0.6 i
24.3 - 1.4 i	28.5 - 0.9 i	39.4 - 0.7 i
80.1 - 0.9 i	55.9 - 0.2 i	42.1 - 0.3 i
80.9 - 0.6 i	61.6 - 0.6 i	59.6 - 0.8 i
82.4 - 0.2 i	61.6 - 0.7 i	
83.2	64.6 - 0.8 i	
116.5 - 0.2 i	127.7 - 0.6 i	
116.8 - 0.6 i	127.7 - 0.5 i	
117.3 - 1.3 i	160.8 - 0.5 i	

FIG. 3. (color online) Energy dependence of the electron transmission coefficient $T(E)$ through a free standing layer for the model system (a) and for graphene (b). The incidence is normal to the layer. Vertical dashed lines in graph (a) indicate the positions of resonances at Γ point from Table I. In both graphs, vertical bars at kinetic energy of 33.1 eV indicate the onset of non-specular reflected beams.

bound states above the vacuum edge, they do not answer the question of what happens with those that do not survive, i.e., do the latter turn into resonances by acquiring a finite lifetime or they disappear at all. This is due to our numerical search for the eigenvalues of the nonlinear eigenproblem (5) having been restricted to the real axis of E, since no decisive numerical procedure exists to either find all complex-valued roots of this problem or to prove their absence. To shed light on that issue, we solve the eigenvalue problem (5) analytically for a reduced size of the $V(\mathbf{G}-\mathbf{G}')$ matrix to make the problem computationally feasible. Using the *Mathematica* symbolic algebra software, we have analytically evaluated the determinant $\Delta(E)$ of the system (5), then consecutively eliminated the square roots in the equation $\Delta(E) = 0$, which made it possible to reduce it to a polynomial equation. All roots of the polynomial (including the complex ones) were then found with no loss of any of them guaranteed. Since spurious zeros were introduced when reducing the equation to the polynomial, the roots were finally sorted to retain only those that satisfied the original equation $\Delta(E) = 0$. This has been done for Γ, K, and M points with the matrix sizes of 19, 13, and 7, respectively. While all true bound states, both below and above the vacuum edge, were found to reproduce those previously obtained numerically, in addition, complex eigenvalues were found. Results of this calculation are collected in Table I.

Eigenenergies in the lower complex half-plane (resonances) physically manifest themselves as features in elastic scattering spectra at the real energies in the vicinity of the complex eigenvalues[23]. In Fig. 3(a) we plot the coefficient of transmission of an electron incident normally onto our model system. The features in the transmission spectrum clearly agree with the resonances' positions listed in the first column of Table I (Γ point). We note that it is resonances, not the bound states, that underlie the singularities in the elastic scattering spec-

tra: Bound states are orthogonal to the scattering states leading to the independence of the two corresponding motions.

Having established the origin of high-energy resonances in the infinitely thin system let us now return to a realistic graphene. Experimentally, the scattering resonances can be observed in low energy electron diffraction. Figure 3(b) shows *ab initio* normal incidence electron transmission spectrum calculated with the augmented-plane-waves (APW) based variational embedding method[28][29]. The *ab initio* spectrum of graphene is similar to that of the model system: Just below the lowermost resonance we find a point of total reflection followed by total transmission just above the resonance. Total reflection from a free-standing monolayer is a rather counterintuitive finding: unlike the well known case of LEED from crystal surfaces, it is not caused by a gap in the energy spectrum of the semi-infinite substrate[30]. Indeed, the electron can freely propagate in the vacuum half-space behind the graphene layer, and the reflection is solely due to the in-plane scattering.

In both $T(E)$ spectra, one can also see a sharp structure due to the emergence of the secondary beams. Both in the model and in the actual graphene it appears as a transmission minimum at the same energy $E_{KIN} = 33.1$ eV, see Fig. 3. Such structures are well known in classical LEED[31,32], and, contrary to the ones found here, they have a purely "structural" origin and do not depend on details of the electronic structure.

By changing the incidence angle one can observe the *scattering band structure* as the dispersion of transmission probability with $\mathbf{k}$. The *ab initio* calculation of $T(\mathbf{k}, E)$ in the directions ΓK and ΓM is presented in Fig. 4(a). The resonance at Γ is seen to split at the off-normal incidence into three branches with a pronounced anisotropic dispersion, which highlights the non-free-electron character of the graphene states at high energies. A high intensity of Umklapp bands is seen as
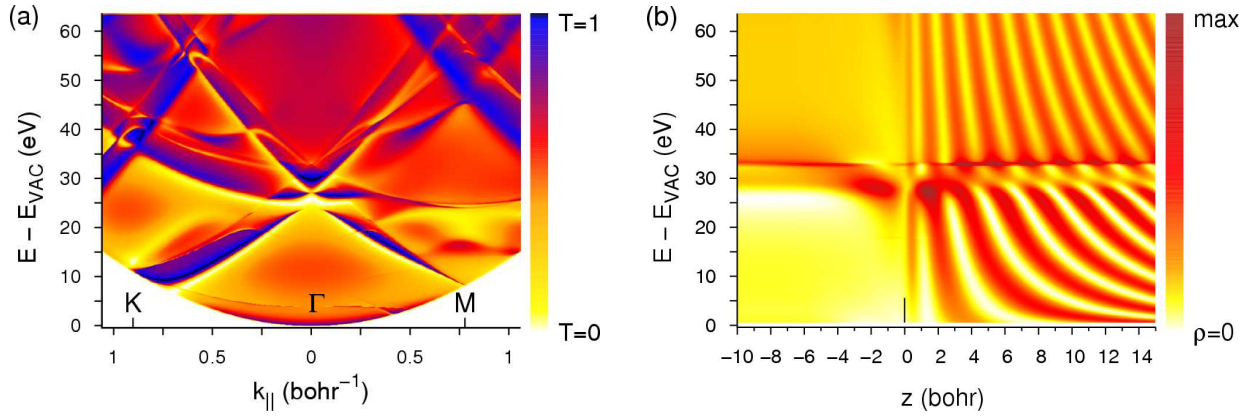
FIG. 4. (color online) (a) Energy-momentum distribution of the transmission probability $T(\mathbf{k}, E)$ through the graphene mono-layer. (b) Energy-dependent density distribution $\rho(z, E)$ in the normal incidence LEED state. Graphene plane is at $z = 0$. The wave is incident from the right; it is normalized as $1 \times \exp(i\mathbf{q} \cdot \mathbf{r})$.

well. To visualize the scattering resonance in real space we present in Fig. 4(b) the energy dependence of the electron density distribution in the LEED state as it comes out of our *ab initio* calculation. The white stripe in the left half-space at $E_{KIN} = 25.5$ eV corresponds to the total reflection, and the vanishing beating in the right half-space at 31.5 eV to the total transmission. The resonance is seen as the pronounced local density enhancement at the graphene layer at 27.5 eV. In perfect accord with our model, it is located between the minimum and the maximum of $T(E)$.

The discovered resonances are, thus, typical of atomic monolayers, and at the surfaces of 3D crystals they may be blurred by the interlayer scattering. For example, in graphite, the resonance falls in a wide gap in the $\mathbf{k} = 0$ projected spectrum, see Fig. 6 in Ref.[33].

These findings suggest important implications on LEED and ARPES from graphene. The two techniques are related by the one-step theory[34,35], according to which the photocurrent is proportional to the probability of the optical transition to the time-reversed LEED state. For the supported graphene, for a sufficiently weak interaction with the substrate, one can, apparently, reduce or enhance the signal from the substrate by tuning the photon energy to the reflection or transmission point. The resonances are rather prominent also at off-normal incidence [Fig. 4(a)]. As they are associated with a strong in-plane scattering it is especially important to be aware of them in studying the corrugated suspended graphene with LEED or ARPES because the resonance area is most strongly affected by the lattice deformation.

Finally, we mention a classical-mechanical analogy of the same effect. Classically, a particle moving along the crystal plane may be scattered away from the plane having collided with an obstacle. In this case, the 'lifetime' of the particle would be the time of flight between two collisions, which for an energetic electron is negligible. We are, however, dealing with a perfectly periodic system with the lattice constant of a few angstroms. The

large lifetimes of the quantum resonances we obtain are due to the coherent quantum scattering and they cannot be accounted for by the classical picture. Moreover, high-symmetry pure bound-states survive, which is impossible classically.

To summarize, we have shown that atomically thin monolayers support resonances of special nature: they originate from a strong coupling of the in-layer scattering to the motion perpendicular to the layer, while each of the two motions, separately, does not support a resonance. For the exactly solvable model of an infinitely-thin crystal we have found the complex eigenvalues of the resonances and demonstrated that they lead to strong sharp structures in the electron diffraction spectra. Another interesting result is that apart from the resonances there exist true bound states immersed in the continuum spectrum, which survive up to high energies above the vacuum level. The purely real eigenvalues are, however, restricted to high-symmetry directions of the 2D Brillouin zone, and they turn into resonances at general $\mathbf{k}$ points.

These general results have found full verification in our *ab initio* calculation of electron diffraction from a realistic free-standing graphene monolayer. The resonance causes a total reflection of the normally incident electron with an energy just below the resonance – a unique phenomenon, as it is caused by purely in-plane scattering.

The thickness of an atomic monolayer is much smaller than the typical mean free path of the photoelectron, so graphene offers a rare opportunity to get rid of the surface sensitivity of photoemission, which is an intrinsic and unavoidable aspect of solid state electron spectroscopies[36]. At the same time, a strong elastic multiple scattering over a wide energy range is retained, producing a well-defined band structure, which can be measured in an angle-resolved experiment. Thus, the studies on the suspended graphene and related structures are expected to shed light on fundamental aspects of spectroscopy, which are blurred in bulk crystals. This concerns, for exam-

ple, inelastic scattering beyond the concept of mean free path, nature of multi-photon transitions[37–39], and the laser streaking of electrons emitted from a solid[40–42]. In this view, the discovered resonances may have important implications for various fields of electron spectroscopy, as they are a general property of atomic monolayers.

* nazarov@gate.sinica.edu.tw

[1] A. H. Castro Neto, F. Guinea, N. M. R. Peres, K. S. Novoselov, and A. K. Geim, Rev. Mod. Phys. **81**, 109 (2009).

[2] D. Golberg, Y. Bando, Y. Huang, T. Terao, M. Mitome, C. Tang, and C. Zhi, ACS Nano **4**, 2979 (2010).

[3] P. Vogt, P. De Padova, C. Quaresima, J. Avila, E. Frantzeskakis, M. C. Asensio, A. Resta, B. Ealet, and G. Le Lay, Phys. Rev. Lett. **108**, 155501 (2012).

[4] L. A. Ponomarenko, F. Schedin, M. I. Katsnelson, R. Yang, E. W. Hill, K. S. Novoselov, and A. K. Geim, Science **320**, 356 (2008).

[5] P. R. Wallace, Phys. Rev. **71**, 622 (1947).

[6] S. Latil and L. Henrard, Phys. Rev. Lett. **97**, 036803 (2006).

[7] P. E. Trevisanutto, C. Giorgetti, L. Reining, M. Ladisa, and V. Olevano, Phys. Rev. Lett. **101**, 226405 (2008).

[8] L. M. Malard, M. H. D. Guimarães, D. L. Mafra, M. S. C. Mazzoni, and A. Jorio, Phys. Rev. B **79**, 125426 (2009).

[9] V. M. Silkin, J. Zhao, F. Guinea, E. V. Chulkov, P. M. Echenique, and H. Petek, Phys. Rev. B **80**, 121408 (2009).

[10] T. Suzuki and Y. Yokomizo, Physica E: Low-dimensional Systems and Nanostructures **42**, 2820 (2010).

[11] E. Kogan and V. U. Nazarov, Phys. Rev. B **85**, 115418 (2012).

[12] A. M. Shikin, G. V. Prudnikova, V. K. Adamchuk, F. Moresco, and K.-H. Rieder, Phys. Rev. B **62**, 13202 (2000).

[13] A. Bostwick, T. Ohta, T. Seyller, K. Horn, and E. Rotenberg, Nat Phys **3**, 36 (2006).

[14] Y. S. Dedkov, M. Fonin, U. Rüdiger, and C. Laubschat, Phys. Rev. Lett. **100**, 107602 (2008).

[15] P. Sutter, M. S. Hybertsen, J. T. Sadowski, and E. Sutter, Nano Letters **9**, 2654 (2009).

[16] I. Pletikosić, M. Kralj, P. Pervan, R. Brako, J. Coraux, A. T. N'Diaye, C. Busse, and T. Michely, Phys. Rev. Lett. **102**, 056808 (2009).

[17] Y. Liu, L. Zhang, M. K. Brinkley, G. Bian, T. Miller, and T.-C. Chiang, Phys. Rev. Lett. **105**, 136804 (2010).

[18] D. Niesner, T. Fauster, J. I. Dadap, N. Zaki, K. R. Knox, P.-C. Yeh, R. Bhandari, R. M. Osgood, M. Petrović, and M. Kralj, Phys. Rev. B **85**, 081402 (2012).

[19] K. R. Knox, A. Locatelli, M. B. Yilmaz, D. Cvetko, T. O. Menteş, M. A. Niño, P. Kim, A. Morgante, and R. M. Osgood, Phys. Rev. B **84**, 115401 (2011).

[20] A. Locatelli, K. R. Knox, D. Cvetko, T. O. Mentes, M. A. Niño, S. Wang, M. B. Yilmaz, P. Kim, R. M. Osgood, and A. Morgante, ACS Nano **4**, 4879 (2010).

[21] P. W. Sutter, J.-I. Flege, and E. A. Sutter, Nat Mater **7**, 406 (2008).

[22] http://elk.sourceforge.net.

[23] L. D. Landau and E. M. Lifshitz, *Quantum Mechanics: The Non-Relativistic Theory* (Butterworth-Heinemann, London, 1981).

[24] All the solutions (3) are even in z (σ bands), which is the consequence of the δ-potential supporting one bound state at most.

[25] G. H. Golub and H. A. van der Vorst, Journal of Computational and Applied Mathematics **123**, 35 (2000).

[26] H. Friedrich and D. Wintgen, Phys. Rev. A **32**, 3231 (1985).

[27] G. Cattapan and P. Lotti, The European Physical Journal B - Condensed Matter and Complex Systems **66**, 517 (2008).

[28] E. E. Krasovskii, Phys. Rev. B **70**, 245322 (2004).

[29] The method employs eigenfunctions of a repeated-slab band structure as basis functions to represent the LEED state. For the present purpose they were obtained with the full-potential linear APW of Ref.[43].

[30] J. C. Slater, Phys. Rev. **51**, 840 (1937).

[31] E. G. McRae, Rev. Mod. Phys. **51**, 541 (1979).

[32] R. Jones and P. Jennings, Surface Science Reports **9**, 165 (1988).

[33] N. Barrett, E. E. Krasovskii, J.-M. Themlin, and V. N. Strocov, Phys. Rev. B **71**, 035427 (2005).

[34] G. D. Mahan, Phys. Rev. B **2**, 4334 (1970).

[35] P. J. Feibelman and D. E. Eastman, Phys. Rev. B **10**, 4932 (1974).

[36] W. Schattke and M. A. van Hove, eds., *Solid-State Photoemission and Related Methods. Theory and experiment* (Wiley-VCH, Berlin, 2003).

[37] H. Petek and S. Ogawa, Progress in Surface Science **56**, 239 (1997).

[38] W. Schattke, E. E. Krasovskii, R. Díez Muiño, and P. M. Echenique, Phys. Rev. B **78**, 155314 (2008).

[39] H. Husser, J. van Heys, and E. Pehlke, Phys. Rev. B **84**, 235135 (2011).

[40] A. L. Cavalieri, N. Mueller, T. Uphues, V. S. Yakovlev, A. Baltuska, B. Horvath, B. Schmidt, L. Bluemel, R. Holzwarth, S. Hendel, M. Drescher, U. Kleineberg, P. M. Echenique, R. Kienberger, F. Krausz, and U. Heinzmann, NATURE **449**, 1029 (2007).

[41] A. K. Kazansky and P. M. Echenique, Phys. Rev. Lett. **102**, 177401 (2009).

[42] E. E. Krasovskii, Phys. Rev. B **84**, 195106 (2011).

[43] E. E. Krasovskii, F. Starrost, and W. Schattke, Phys. Rev. B **59**, 10504 (1999).